Clays and Clay Minerals, Vol. 62, No. 3, 188–202, 2014.

THE INTERACTION BETWEEN BENTONITE AND WATER VAPOR. I: EXAMINATION OF PHYSICAL AND CHEMICAL PROPERTIES

Michel Heuser[1], Christian Weber[1], Helge Stanjek[1], Hong Chen[2], Guntram Jordan[3], Wolfgang W. Schmahl[3], and Carsten Natzeck[4]

[1] Clay and Interface Mineralogy, RWTH Aachen University, Bunsenstrasse 8, 52072 Aachen, Germany,
[2] Department of Materials Technology, Flemish Institute for Technological Research (VITO), Boeretang 200, B 2400 Mol, Belgium
[3] Department for Geo- and Environmental Sciences, Ludwig-Maximilians-Universität München (LMU), Theresienstrasse 41, 80333 Munich, Germany
[4] Institute of Functional Interfaces, Karlsruhe Institute of Technology (KIT), Hermann-von-Helmholtz-Platz 1, 76344 Eggenstein-Leopoldshafen, Germany

Abstract—The influence of water vapor on bentonites or smectites is of interest in many different fields of applied mineralogy such as nuclear-waste sealing or casting in the foundry industry. The water vapor affects the smectite surface and perhaps its structure probably leading to mostly unfavorable changes in its properties. In this first part of the present study, the influence of hot water vapor (200ºC) on the physico-chemical and mineralogical properties of smectite-group minerals was studied. After the steam treatment, turbidity measurements, methylene-blue sorption, water adsorption, and cation exchange capacity (CEC) were measured on both untreated and treated samples. Mineralogical changes were monitored by X-ray diffraction (XRD) and X-ray photoelectron spectroscopy (XPS) was used to measure O, Al, and Si. Only a few parameters showed differences between the untreated and vapor-treated samples. Sedimentation volumes (SV) decreased following the treatment. As shown by XRD and XPS, the crystalline structure of smectite remained unaffected by the steam treatment. Equivalent sphere diameters (ESD) were not affected systematically by the steam treatment. Differences in CEC values between untreated and treated samples were observed, but only for smectites with monovalent interlayer cations. From the variety of different measurements the conclusion of the present study was that steam treatment changes the charge properties at or near the smectite particle surface.

Key Words—Cation Exchange Capacity, Equivalent Sphere Diameter, Methylene Blue Sorption, Water Vapor, XPS, XRD.

INTRODUCTION

The industrial and technical applications of clay minerals and bentonites include geotechnical use in contaminant removal (Viraraghavan and Alfaro, 1996; Mellah and Chegrouche, 1997; Gitipour *et al.*, 1997), drilling or reinforcing fluids (Erdoğan and Demirci, 1996; Luckham and Rossi, 1999), landfill technology (Ashmawy *et al.*, 2002; Scalia and Benson, 2011), ceramics in material science (Zhu *et al.*, 2002; Fahrenholtz, 2008), and molding in foundry technology (Baier, 1991; Beeley, 2001).

By definition, bentonites contain >50 wt.% of smectite-group minerals such as montmorillonite or beidellite (Grim and Güven, 1978; EUBA, 2006; Murray, 2007). For foundry applications, smectite contents of >70 wt.% are preferred (Grefhorst, 2006). Additional minerals include quartz, feldspars, micas, kaolinite, anatase, cristobalite, opal, and volcanic glasses (Ufer *et al.*, 2008; Christidis and Huff, 2009). The physical and chemical properties of bentonite vary with the amount of smectite and mainly with its parameters such as particle size and morphology, hydration state of the interlayer cations, and the presence of free water in the pore space (Montes-H. *et al.*, 2003; Kaufhold *et al.*, 2010).

With regard to foundry technology, molding or green sand consists of refractory material, usually quartz (for special applications zircon or chromite sand is used), bentonite as a binder, special additives such as lustrous carbon producers, and water (Träger and Bührig-Polaczek, 2000; Beeley, 2001; Recknagel and Dahlmann, 2008). Smectite in contact with water encloses the surface of quartz particles and contributes to the plasticity and stability of molding sand. During the casting process, liquid water in the molding sand evaporates near the molten metal to an exceedingly hot vapor moving along the temperature gradient to cooler regions, condensing to liquid water. This region, known as the 'condensation zone', is characterized by water contents greater than they were at the beginning of the casting process (Grefhorst *et al.*, 2005; Jordan *et al.*, 2013). During this transport process water vapor affects the smectite particles and probably their surface properties. This potential modification might be a controlling factor leading to poor quality molding sands.

* E-mail address of corresponding author:
michel.heuser@cim.rwth-aachen.de
DOI: 10.1346/CCMN.2014.0620303

The influence of water vapor on bentonite is also important for the sealing of nuclear-waste repositories. Several decades of research has resulted in a detailed understanding of the influence of water vapor on the geotechnical and mineralogical parameters of bentonite. A vapor treatment was performed at temperatures between 150 and 250ºC by Couture (1985a, 1985b). Both permeability and its ability to swell and to fill fractures decreased significantly up to 250ºC. The reduction in swelling capacity commenced at 150ºC.

A decrease in swelling capacity was also observed (Oscarson and Dixon, 1989) which was not caused by an alteration of the mineralogical composition of the montmorillonite and which was influenced by physical aggregation of clay particles, only to a lesser extent. The permeability of unprocessed and treated bentonites was discovered to be different (Oscarson *et al.*, 1990) but those authors gave no reasons why this was so. Both studies have in common that differences between unprocessed and treated bentonites were observed for water-vapor treatments starting at 110ºC. The positive aspects of untreated bentonites (such as fast swelling and low water permeability) were lost.

A steam treatment at temperatures >260ºC was performed by Güven (1990) resulting in a modified microstructure and a disturbance of the lamellar fabric.

The influence of steam on bentonite at temperatures of <120ºC was assessed by Madsen (1998). Analyses by XRD, infrared spectroscopy (IR), and thermogravimetry showed no significant changes due to steam treatment except for a slight increase in CEC. The reduction of swelling pressure was attributed to aggregation of clay particles.

The effects of steam on the surface properties of two sodium-smectites were studied by Bish *et al.* (1997). No structural mineralogical changes (XRD) after treatment were observed. Based on ^{27}Al magic angle spinning-nuclear magnetic resonance (MAS-NMR) measurements, those authors speculated about a relocation of Al, but the differences between spectra of untreated and vapor-treated samples were few. Contact angles determined with polar liquids were noted to change after steaming, however, whereas non-polar liquids did not show any modification of the contact angles. The water-adsorption isotherms of untreated and steam-treated samples differed and the ability of samples to adsorb water decreased, although with hysteresis effects. A small increase in zeta potentials after the treatment was detected.

The influence of water vapor on bentonite over the temperature range 90–110ºC led to bulk-clay expansion and aggregation (Pusch, 2000). The hydration rate and swelling pressure were of the same order of magnitude for untreated and steam-treated clay, however. The hydraulic conductivity increased by up to 10% due to a more heterogeneous microstructure after the treatment. Partial dissolution of smectite and precipitation of Si or silica after cooling following the treatment induced aggregation and cementation of particles. The Si and Al concentrations were not measured in the present study, however. Changes in the physical properties were insignificant.

In summary, the following effects with steam treatment were observed: (1) the ability to swell and the swelling pressure decreased; (2) the permeability and hydraulic conductivity increased; (3) the CEC increased slightly; (4) no structural changes were evident from studies using XRD, IR, or thermogravimetry.

Based on the results of the studies cited above and their interpretation, the mechanisms and processes of steam/smectite interactions and changes at particle level are still not understood fully. The causes of apparent changes in surface properties after steaming, exemplified by contact-angle and zeta-potential measurements (Bish *et al.*, 1997), are unclear. The focus of the present work was to understand the processes in the system involving hot steam and smectite.

MATERIAL AND METHODS

Five industrial bentonites used for foundry applications (Bentonite C, D, E, H, and W abbreviated hereafter as BeC, BeD, BeE, BeH, and BeW) and two commercial clays (Namorit S and Volclay) were used. The mineralogical characterization of samples is presented below in the section on XRD. The sample-preparation steps were: (1) Ultrasonic dispersion of raw material in deionized water to a concentration of 5 wt.%. (2) Enrichment of smectite by separating the <2 μm fraction by Atterberg sedimentation. (3) Preparation of homoionic forms by washing 10 g of sample material under continuous stirring in 600 mL of a 3 M salt solution of NaCl, KCl, $MgCl_2$, or $CaCl_2$, respectively. After ~36 h the stirrer was switched off, and the particles sedimented. The clear supernatant was removed and replaced by a new 3 M salt solution. This procedure was repeated six times. Bentonites C, D, E, H, and W were prepared in the four forms, Namorit S and Volclay only in the Mg- and Na-species respectively. (4) Dialysis in Roth-Nadir dialysis tubing with a diameter of 50 mm and a pore size of 2.5–3.0 nm to remove the remaining free salts in the clay dispersion. Dialysis was completed when the electrical conductivity of the clay dispersion in the dialysis tubing was <20 μS/cm. (5) Freeze drying of sample material and storage in airtight PVC containers.

The steam treatment was performed in Berghof digestion autoclaves (Figure 1). Deionized water and sample material were poured into the polytetrafluoroethylene (PTFE) insert. The sample insert was placed in the water insert and closed with a lid. Both inserts were placed in the steel body and closed. Steam treatments were performed at 200ºC in an oven for a period of 6 days. Note that the sample had no contact with liquid water during the steam process. For all experiments a smectite-to-water ratio of 1:20 was used. After the treatment the closed autoclaves were cooled for 24 h.

https://doi.org/10.1346/CCMN.2014.0620303 Published online by Cambridge University Press

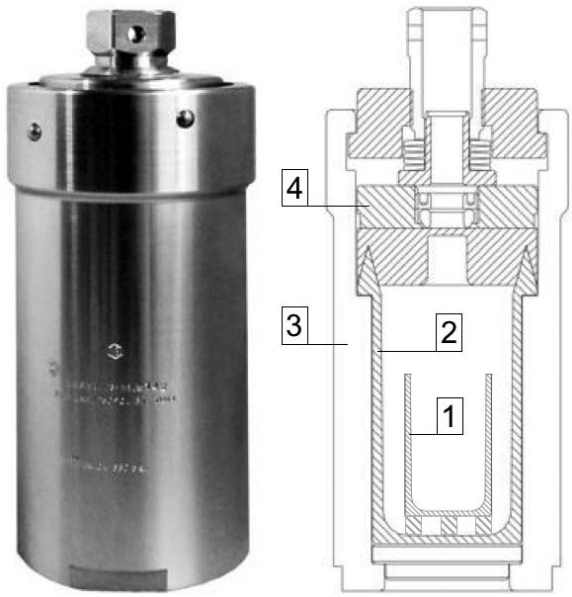

Figure 1. Pressure digestion vessel made of high-alloy stainless steel SS 316 Ti, max. 200 bar, max. 250ºC (Berghof autoclave DAB-3). (Left) Image of stainless steel body with lid; (right) cross section (modified after Berghof, 2012). The autoclave consists of four main components: (1) 50 mL PTFE insert for the sample; (2) 250 mL PTFE insert for the water with lid; (3) high-alloy stainless steel body with bayonet lock; and (4) rupture disc to limit maximum pressure reliably.

Having reached room temperature the clear supernatant was removed for further analysis; the solid was dried at 200ºC for ~1 h, held in a desiccator, and stored in airtight PVC containers.

In order to examine the physico-chemical differences between untreated and steam-treated bentonite samples, laboratory tests were performed as listed below. For all experiments only the <2 μm clay fraction was used.

SOLUTION CHEMISTRY

The ionic composition of the supernatant water after steaming may provide an indication of possible dissolution processes due to the steam treatment. The supernatant was analyzed by ion chromatography (IC 850 Professional, Metrohm, Germany) for anions F^-, Br^-, Cl^-, NO_2^-, NO_3^-, SO_4^{2-}, and PO_4^{3-}, and cations Li^+, NH_4^+, K^+, Na^+, Cs^+, Mg^{2+}, and Ca^{2+}. The lower detection limit was 0.5 mg/L for all ions. The deionized water (Table 1, sample #1) was essentially free of any contamination. For the second test (#2) only water was added to the autoclaves, whereas the standard test procedure remained unchanged. In order to quantify removable ions for the untreated sample, bentonite material was dispersed in deionized water (1:70) and kept in dispersion for five days (#3). After sedimentation, clear supernatant was filtered (0.45 μm) and concentrations of common ions were determined. The last test (#4) represents the standard steam treatment, where the water in the autoclaves was analyzed after steaming.

In order to check if water vapor affects tetrahedral or octahedral sheets, Si and Al were measured in the supernatant. To check whether the concentrations of Al and Si were to be ascribed to the steam treatment, blank experiments were performed. One gram (1 g) of sample was dispersed in 20 mL of deionized water and kept in dispersion for 5 days; the Al and Si concentrations were determined in the clear supernatants. Background concentrations, c_0, of Al ($c_{0,Al}$ = 0.4 mg/L) and Si ($c_{0,Si}$ = 0.1 mg/L) were measured in deionized water and subtracted from sample concentrations.

Silicon was measured by the molybdenum blue method according to Köster (1979, p. 39) at a wavelength of 650 nm. Aluminum was measured using the aluminon red method according to Köster (1979, p. 51) at a wavelength of 530 nm. The relative uncertainties in concentrations are 3 and 0.3% for Al and Si, respectively (Köster, 1979). An UV-VIS spectrophotometer (Specord 210 Plus, Analytik Jena, Germany) was used to perform photometric measurements.

Colorimetry

The change in color in the course of steam treatment was quantified by colorimetry using a Chroma meter

Table 1. Ion concentrations in supernatant water after treatment in selected experiments (three replicates each).

#	Cation [mg/L]	K^+	Na^+	NH_4^+	Mg^{2+}
1	Unprocessed water	0	0	0	0
2	Treated water	0.61	0.93	4.29	0
3	BeW, Mg dispersed in water (1:70)	1.37±0.01	0.77	<0.20	4.32±0.18
4	BeW, Mg, steam-treated	1.18±0.06	1.94±0.18	9.36±0.66	0
#	Anion [mg/L]	F^-	Cl^-	NO_3^-	SO_4^{2-}
1	Unprocessed water	0	0	0	0
2	Treated water	0.47	0.86	0	0.44
3	BeW, Mg dispersed in water (1:70)	0	0.79±0.01	0.85±0.24	0.50±0.09
4	BeW, Mg, steam-treated	2.26±0.19	1.08±0.67	0	0.80±0.27

https://doi.org/10.1346/CCMN.2014.0620303 Published online by Cambridge University Press

(CR-400, Konica Minolta, Germany). In the $L^*a^*b^*$ color space (DIN 6174), L^* describes the brightness (luminance) of color, which ranges between 0 (black) and 100 (white). The parameter a^* can range between −150 and +100, where negative values indicate a green and positive ones a red color. The parameter b^* may vary between −100 (blue) and +150 (yellow). Relative uncertainty on L^*, a^*, and b^* is <±1%, according to the Chroma meter manual.

Sedimentation volume (SV)

One gram (1 g) of sample material dispersed in 56 mL of deionized water was poured into graduated cylinders. After adding 3 g of $MgCl_2 \cdot 6H_2O$ (Merck, Germany) to the clay dispersion to facilitate flocculation, the cylinders were shaken and left to sediment for 1 day. The sedimentation volume is given in percent in relation to the initial volume of 56 mL. The test procedure was described by Oscarson and Dixon (1989).

Water adsorption (WA)

Water adsorption or water-uptake capacity is used widely in quality control for industrial clay minerals and bentonites. The water adsorption of untreated and steam-treated bentonites was determined using the method and instrumentation described by Dieng (2005), itself a modification of the Enslin-Neff method (Neff, 1959). For the test, 0.2 g of dry sample material (oven-dried at 200ºC) was brought into direct contact with liquid water. The measurement lasted for 24 h, a time period in which evaporation could be ignored. The relative uncertainty in the water adsorption was ±2.5% (Dieng, 2005).

Cation exchange capacity (CEC)

In order to obtain information about charge conditions in the interlayer of smectite and their change due to steaming, the CEC was determined using the copper(II)-triethylenetetramine (CuTrien) method after Meier and Kahr (1999). For the experiment, 100 mg of sample material was dispersed in 50 mL of deionized water by shaking. Then 2 mL of a 0.1 mol/L Cu-Trien solution, made from $CuSO_4 \cdot 5H_2O$ (Merck, Germany) and triethylene tetramine (>97% purity, Sigma Aldrich, Germany) was added. After 1 h, the dispersion was filtered (pore size of the filter 0.45 μm) and its absorption measured using an UV-VIS spectrophotometer (Specord 210 Plus, Analytik Jena, Germany) at 577 nm (max. absorption of the CuTrien solution). The relative uncertainty in the CEC measurements was ±3%.

Equivalent sphere diameter (ESD)

To determine whether the steam treatment leads either to particle growth or to particle dissolution, equivalent sphere diameters (ESD) of untreated and treated smectites were calculated from turbidity measurements of dispersions having increasing concentrations of solid. Turbidity values can be related to ESD values using the Mie theory of light scattering (Lange, 1968, 1969; Melik and Fogler, 1983; Lange, 1995; Lagaly *et al.*, 1997). One hundred and fifty milligrams (150 mg) of sample material was dispersed in 150 mL of deionized water by ultrasonic treatment (5 min). An aliquot of 0.1 mL was added to 50 mL of deionized water and the dispersion homogenized by a peristaltic pump in a loop including a flow-through cuvette. After measuring absorption at 850 nm, the next aliquot of 0.1 mL was added to the dispersion. This procedure was repeated 20 times, resulting in a total of 20 measurements at increasing concentrations. An UV-VIS spectrophotometer (Specord 210 Plus, Analytik Jena, Germany) was used to measure the absorption.

In order to calculate the particle size, the measured absorption is converted into turbidity according to equation 1, where L is the scattering length of the cuvette (L = 1 cm) and D is the measured absorption (Lagaly *et al.*, 1997):

$$\tau = 2.303 \cdot (D/L) \quad (1)$$

A plot of the clay-water-solution concentration (c) *vs.* the calculated turbidity (τ) should result in a linear function with a slope $\partial\tau/\partial c$.

$$r_{\text{particle}} = \left(\frac{\left(\frac{\tau}{c}\right) \cdot \lambda^4 \cdot \rho}{32 \cdot \pi^4 \cdot n_{\text{fluid}}^4 \cdot \left(\frac{m^2-1}{m^2+2}\right)^2} \right)^{1/3} \cdot 10^7 \quad (2)$$

with $m = n_{\text{solid}}/n_{\text{fluid}}$.

Equivalent sphere radii (r_{particle} in nm) were obtained from the averages of 20 measurements (equation 2 of Lagaly *et al.*, 1997). The wavelength of the photometer is $\lambda = 8.5 \times 10^{-5}$ cm, ρ = 2.6 g/mL is the density of the mineral, n_{fluid} = 1.33 is the refractive index of the fluid (deionized water), and n_{solid} = 1.59 (Lagaly *et al.*, 1997, p. 288) is the refractive index of the solid phase. A slightly smaller n_{solid} was chosen, however, because newer literature (Anthony *et al.*, 2013) provided values of n down to 1.51 for montmorillonite. The absolute error of ESD measurements ranges between 0.5 and 9.0 nm.

Methylene blue absorption (MBS)

The interaction of dye molecules like methyl orange or methylene blue with clay minerals has been studied extensively (Kahr and Madsen, 1995; Bujdák *et al.*, 2001; Jacobs and Schoonheydt, 2001; Ma *et al.*, 2004; Czímerová *et al.*, 2004). The determination of the smectite content in bentonites by methylene blue absorption is a standard method in quality control in foundry technology (Grefhorst, 2006; VDG P35).

For the test, 50 mg of sample material was dispersed in 70 mL of deionized water by ultrasonic treatment for 5 min. Subsequently, 8 mL of a 1.25×10^{-4} mol/L methylene blue solution (Clin-Tech Ltd., United Kingdom) was added. Absorption spectra of clay-dye

https://doi.org/10.1346/CCMN.2014.0620303 Published online by Cambridge University Press

dispersions were measured between 400 and 800 nm using an UV-VIS spectrophotometer (Specord 210 Plus, Analytik Jena, Germany). A single experiment lasted for 20 h during which spectra were recorded every 15 min.

X-ray diffraction (XRD)

X-ray diffraction patterns were measured using a Bruker D8 Advance θ-θ diffractometer (CuKα radiation generated at 40 mA and 40 kV) with a variable divergence slit width set to 12 mm sample length and a receiving slit width of 0.2 mm. The Rietveld program BGMN (Bergmann and Kleeberg, 1998) was used to determine the quantitative mineralogical composition of non-oriented powder samples (<2 μm). All samples were analyzed from 2 to 92º2θ with a measuring time of 3 s per step.

X-ray photoelectron spectroscopy (XPS)

XPS was chosen in order to check for a possible change of the internal chemical structure after steam treatment. Specimens were prepared as films from a 1 wt.% dispersion of <2 μm Volclay-Na, BeC-Ca, BeD-Mg, and BeH-K in deionized water. Aliquots of the dispersion were withdrawn using a pipette and distributed carefully over a petrographic microscope glass slide. After evaporation of residual water the specimens were dried at 200ºC and kept in a desiccator until analysis.

Angle-resolved XPS measurements of Volclay-Na were carried out on a Thermo Theta Probe spectrometer (Thermo Fisher Scientific, USA). The incident beam consisted of monochromatic AlKα radiation with a photon energy of E = 1486.6 eV. Step width and spot size were defined as 0.1 eV and 400 μm, respectively. In the case of Al_{2p} and Si_{2p} measurements, dwell time was set at 200 ms and 400 scans were performed for each angle. The O_{1s} line was recorded with a dwell time of 100 ms and 10 scans per angle.

Further angle-resolved XPS measurements of BeC-Ca, BeD-Mg, and BeH-K were carried out on an XPS/AES/UPS-system by PREVAC sp. z o.o. (Poland) with a Hemispherical Analyzer R4000 from VG Scienta Ltd. (UK). The incident beam consisted of non-monochromatic AlKα radiation. All lines of Al_{2p}, Si_{2p}, O_{1s}, and C_{1s} were recorded at five scans per angle. Step width and dwell time per step were defined as 0.05 eV and 100 ms, respectively; the pass energy of the analyzer was fixed at 100 eV.

The angle of the incident beam was either 38º or 68º, measured against the vertical direction. During all experiments a flood-gun was used for charge compensation.

RESULTS

XRD

Bentonites C–W (<2 μm fraction) are almost pure smectites, with a very small anatase content (<1%). Volclay consists of smectite (91%), halite (7%), and quartz (2%); Namorit-S consists of smectite (93%), kaolinite (6%), and anatase (<1%). No changes in peak positions were observed after steaming. The lattice constant b, which is sensitive especially to Fe contents in octahedral sites, did not change after the treatment (Heuser *et al.*, 2013). Minor differences in peak intensities between untreated and treated samples were observed for the (001) reflection of smectite (Figure 2). These differences are assumed to result from sample preparation (texturing) and are, therefore, considered insignificant.

The comparison of peak positions of different samples is possible because humidity and storage time were the same for untreated and treated samples. After drying at 200ºC, the samples were stored in PVC containers and measured with XRD after 1–2 weeks. The XRD measurements took ~8 h, during which the samples were exposed to room temperature and humidity. However, this time period would be sufficient to create similar hydration states for untreated and treated samples.

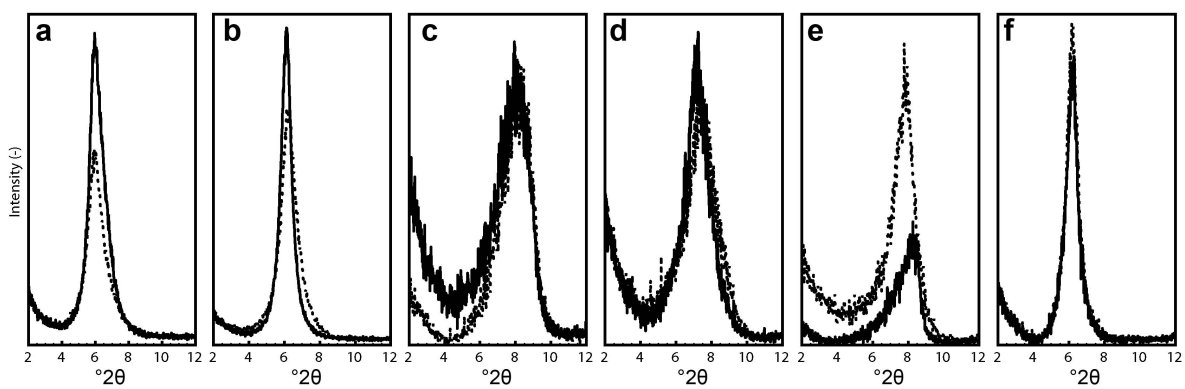

Figure 2. (001) reflection of smectite: (a) bentonite D-Ca; (b) bentonite D-Mg; (c) bentonite D-K; (d) bentonite D-Na; (e) Voclay-Na; and (f) Namorit S-Mg. The solid line represents the untreated sample, the dotted line the steam-treated sample.

https://doi.org/10.1346/CCMN.2014.0620303 Published online by Cambridge University Press

Table 2. Si concentration in the supernatant water after the treatment and in 1 g of sample material dispensed in 20 mL of deionized water after filtration (0.45 μm filter).

Si (mg/L)	Supernatant water after treatment	1 g of untreated material dispersed in 20 mL of deionized water
Deionized water	0.085	–
Namorit S	4.742	31.26
BeH-Ca	0.492	9.704
Volclay	5.766	35.42

Ionic inventory

In all samples, lithium, cesium, and calcium, as well as bromide, nitrite, and phosphate, were below the ion chromatography detection limit of 0.5 mg/L (Table 1). In general, all concentrations were in the lower mg/L range. Differences between the four samples can be assigned to measurement uncertainties and a low contamination by PTFE inlets of the autoclaves as shown by test #2.

The Al concentrations in the blank samples and the steam-treated supernatant did not exceed the concentrations found in untreated deionized water. For Si, the steam treatment consistently reduced the concentrations relative to those of the dispersions made from untreated samples (Table 2).

Colorimetry

Color measurements confirmed the visual impression, which did not reveal any differences between untreated and treated smectites.

Sedimentation volume

The sedimentation volume (SV) represents the maximum volume captured by unconfined clay in suspension after a fixed time. The influence of water vapor on the sedimentation volume of montmorillonite depends on the temperature of the vapor and the moisture in the system. In order to verify these results, the specific volume of selected untreated and steam-treated samples was quantified. Sedimentation volumes of treated samples were always smaller than those of treated samples, which was ascribed to a change in swelling capacity of smectite (Oscarson and Dixon, 1989). A linear relationship between untreated and treated samples was found (Figure 3), although with a low correlation factor of $R^2 = 0.66$.

Water adsorption

Water adsorption varies substantially as a function of the interlayer cations of smectite (*e.g.* Montes-H. *et al.*, 2003; Montes-H. and Geraud, 2004). Moreover, a clear

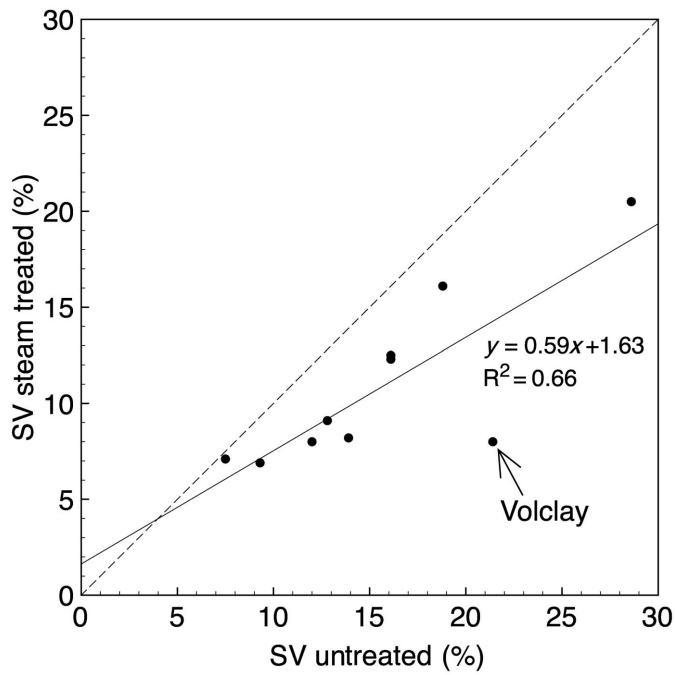

Figure 3. Sedimentation volume (SV) of selected samples after 1 day of sedimentation: results are presented as percentages of the initial volume (56 mL). Dotted line: $y = x$; full line: linear regression (see text for explanation).

https://doi.org/10.1346/CCMN.2014.0620303 Published online by Cambridge University Press

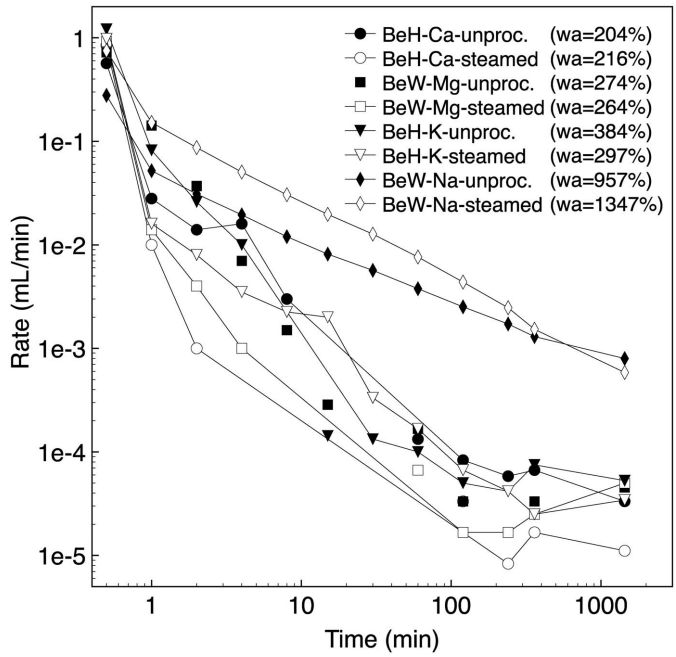

Figure 4. Rates of water adsorption *vs.* time of selected samples and interlayer cations. The values in parentheses represent the water adsorption (wa, %) after 24 h.

distinction between monovalent and divalent interlayer cations was observed. Due to changes in the width of the filling area on the filter plate of the experimental equipment and the dependence of water adsorption on the interlayer cation of smectite, samples adsorbed different amounts of water at the beginning of the experiments (Figure 4). With increasing time, the water adsorption of treated and untreated samples differed by more than the experimental error of 2.5% (Dieng, 2005). Differences in water adsorption between untreated and treated samples (Figure 4, values in parentheses) are significant, therefore. In contrast, water-adsorption rates showed differences at the beginning of the test only. After 30–60 min, the rates of adsorption by untreated and treated samples were identical within uncertainty and converged rapidly toward zero.

Cation exchange capacity

The CEC of some samples decreased while for others it remained unchanged after the steam treatment. The CEC values of untreated and treated samples did not correlate with each other (Figure 5). Furthermore, the kind of smectite had no influence on the CEC, but the interlayer cation of the smectite did (Figure 5a,b). Samples saturated with divalent cations showed little or no change in CEC, whereas samples with monovalent cations reacted to steaming. For most of the samples, the CEC values of K-smectites plot below the CEC values of Na-smectites (Figure 5b). The pH of clay dispersions for the CuTrien-method was approximately equal for all untreated and treated samples and ranged between pH 6 and 7.

Equivalent sphere diameter

Sodium-exchanged smectites had smaller ESD values than smectites exchanged with other cations. Aggregation during oven drying after steaming and destruction of aggregates during sonication of particles in water could explain the scattering of ESD measurements above and below the 1:1 line. The treatment itself, however, did not lead to any systematic trend. Neither the variety of smectite (Figure 6a) nor the variety of interlayer cation (Figure 6b) provided a distinction.

Methylene blue absorption

The spectra of methylene sorption experiments showed band positions at 577±4, 614±9, 675±6, and 768±4 nm (Figure 7), which changed both with time and with interlayer cation. The vapor treatment had no noticeable effect on the band positions. The intensity of the bands, however, depended heavily on the type of interlayer cation (Czímerová *et al.*, 2004), especially in terms of the number of bands and their positions. Samples with a divalent cation in the interlayer space (Figure 7a, b, f) showed only one characteristic band at 577±4 nm. On the other hand, samples with a monovalent interlayer cation (Figure 7c, d, e) showed minor differences in intensities after steaming, but no shift in position. The pure methylene blue solution showed two characteristic bands at 616 nm and 668 nm. Both bands are clearly visible within the spectra of monovalent interlayer cations after 30 min as well as after 1200 min. In contrast, spectra of samples with a divalent cation in the interlayer only show remains of the two methylene blue peaks. Sorption rates of methylene blue for

https://doi.org/10.1346/CCMN.2014.0620303 Published online by Cambridge University Press

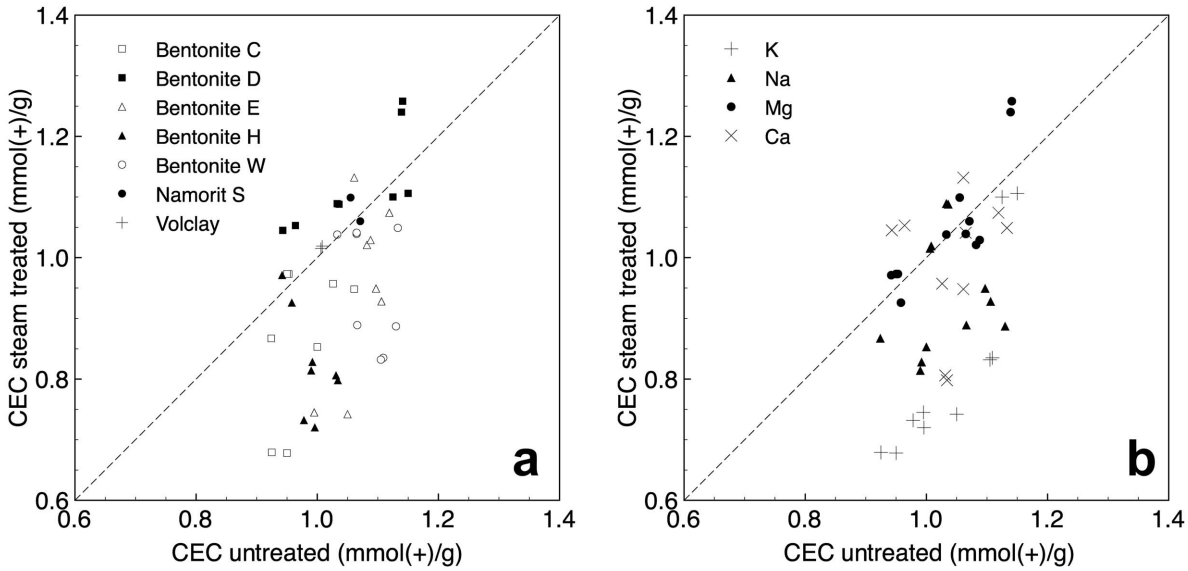

Figure 5. Comparison between the CEC of untreated and steam-treated smectites, sorted by bentonite species (a) and interlayer cation (b).

monovalent cations were almost instantaneous, whereas for divalent cations it took 5−10 min before equilibrium was reached.

XPS

The XPS peaks of Volclay-Na were fitted, after a linear background subtraction, by Gaussian peak-profiles using *Fityk* (Wojdyr, 2010). Unfortunately, no reference line was measured here which makes quantification and direct comparison of binding energies impossible. Nonetheless, qualitative information regarding differences between samples can be obtained by comparing distances between peak centers of species A and B, Δ(AB), according to equation 3:

$$\Delta(AB) = (\text{center}_A - \text{center}_B)_{\text{treated}} - (\text{center}_A - \text{center}_B)_{\text{untreated}} \quad (3)$$

Differences in binding energies, Δ(AB), as calculated from equation 3, are, in all cases, <0.07 eV.

After a linear subtraction of a Shirley background, XPS peaks of BeC-Ca, BeD-Mg, and BeH-K were fitted by Gaussian/Lorentz peak-profiles using *CasaXPS* (Fairley, 2009) and the characteristic peak parameters obtained from all fits were listed (Table 3).

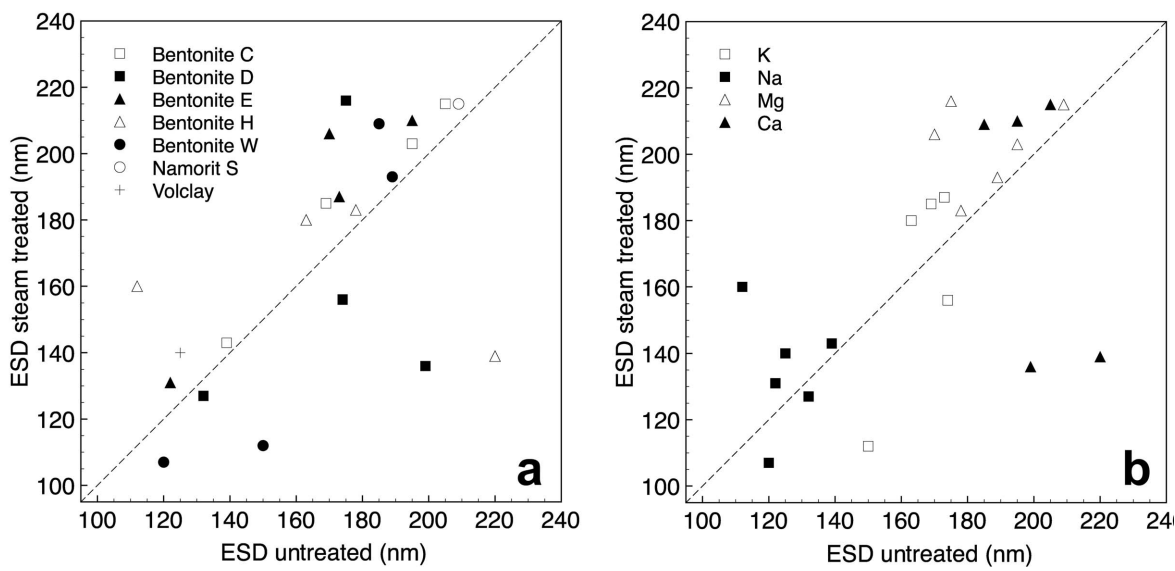

Figure 6. Comparison between ESD values of untreated and steam-treated smectites, sorted by bentonite species (a) and by interlayer cation (b).

https://doi.org/10.1346/CCMN.2014.0620303 Published online by Cambridge University Press

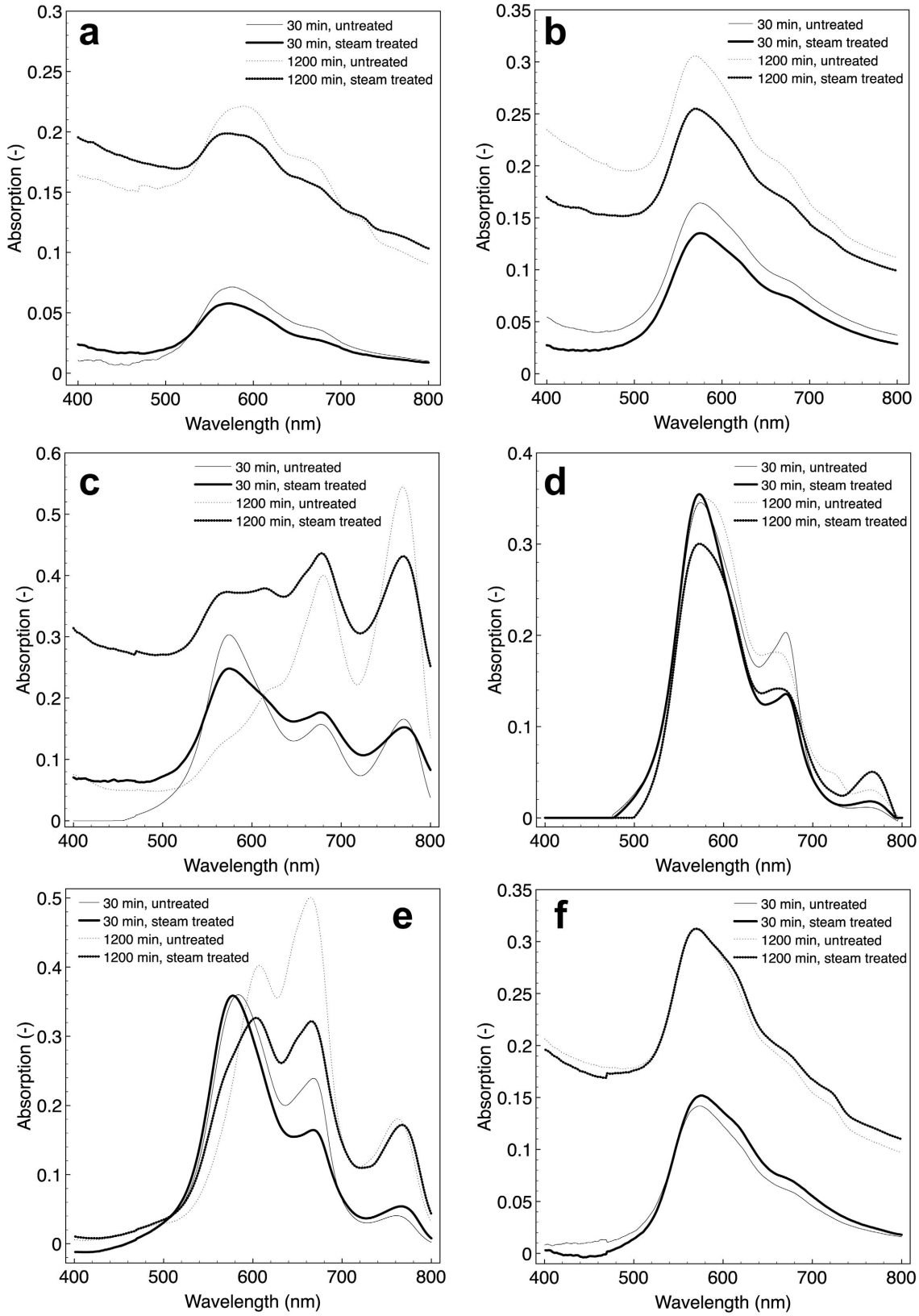

Figure 7. Methylene blue spectra of bentonite D: (a) -Ca, (b) -Mg, (c) -K, (d) –Na, (e) -Volclay-Na, and (f) -Namorit S-Mg, 30 min and 1200 min after the start of the experiment.

https://doi.org/10.1346/CCMN.2014.0620303 Published online by Cambridge University Press

Table 3. Characteristic peak parameters of fitted XPS peaks at working angles of 38º and 68º for untreated and steam-treated samples.

Volclay-Na	38º			68º		
Untreated	Al_{2p}	Si_{2p}	O_{1s}	Al_{2p}	Si_{2p}	O_{1s}
Center [eV]	74.2	102.4	531.7	74.2	102.3	531.6
Height [cps]	120.17	455.12	2718.16	58.63	232.72	1585.25
FWHM [eV]	1.65	1.78	1.94	1.68	1.81	1.97
Treated	Al_{2p}	Si_{2p}	O_{1s}	Al_{2p}	Si_{2p}	O_{1s}
Center [eV]	74.4	102.6	531.9	74.4	102.5	531.9
Height [cps]	107.89	417.95	2507.06	54.44	218.93	1504.50
FWHM [eV]	1.94	2.02	2.18	1.96	2.04	2.22
BeC-Ca	38º			68º		
Untreated	Al_{2p}	Si_{2p}	O_{1s}	Al_{2p}	Si_{2p}	O_{1s}
Center [eV]	74.4	102.5	531.7	74.3	102.4	531.6
Height [cps]	69721	191144	922851	63722	172170	775608
FWHM [eV]	1.98	2.21	2.39	1.94	2.11	2.38
Treated	Al_{2p}	Si_{2p}	O_{1s}	Al_{2p}	Si_{2p}	O_{1s}
Center [eV]	74.4	102.6	531.7	74.4	102.6	531.6
Height [cps]	64580	156029	688327	54307	130362	569123
FWHM [eV]	2.26	2.57	3.05	2.67	2.77	3.06
BeD-Mg	38º			68º		
Untreated	Al_{2p}	Si_{2p}	O_{1s}	Al_{2p}	Si_{2p}	O_{1s}
Center [eV]	74.4	102.5	531.6	74.3	102.4	531.5
Height [cps]	65972	178281	812361	54070	137681	585774
FWHM [eV]	2.07	2.26	2.53	2.35	2.46	2.73
Treated	Al_{2p}	Si_{2p}	O_{1s}	Al_{2p}	Si_{2p}	O_{1s}
Center [eV]	74.2	102.3	531.5	74.2	102.3	531.3
Height [cps]	68431	181651	844522	58304	147363	625588
FWHM [eV]	2.30	2.52	2.79	2.66	2.58	3.08
BeH-K	38º			68º		
Untreated	Al_{2p}	Si_{2p}	O_{1s}	Al_{2p}	Si_{2p}	O_{1s}
Center [eV]	74.2	102.4	531.5	74.0	102.3	531.4
Height [cps]	75735	218156	1246495	46541	122185	522195
FWHM [eV]	2.02	2.13	2.37	2.22	2.46	2.67
Treated	Al_{2p}	Si_{2p}	O_{1s}	Al_{2p}	Si_{2p}	O_{1s}
Center [eV]	74.2	102.5	531.5	74.1	102.3	531.4
Height [cps]	64896	148288	730853	60044	166322	794525
FWHM [eV]	2.02	2.12	2.43	2.05	2.33	2.48

For these measurements, Carbon C1s at 284.6 eV was used as a reference for a direct comparison of binding energies. After calibration of all binding energies in relation to this reference, the deviation of binding energies was no more than ±0.1 eV.

As the precision of binding-energy determination is generally estimated to be 0.1 eV (Canesson, 1982; Paterson and Swaffield, 1994), the rather small shifts in peak positions are interpreted to be insignificant. From these results the steam treatment is interpreted not to have altered the binding energy of the species investigated.

DISCUSSION

Several laboratory tests were performed to demonstrate and to quantify the influence of hot water steam on

https://doi.org/10.1346/CCMN.2014.0620303 Published online by Cambridge University Press

smectite. Most of the experiments showed no systematic trend between vapor-treated and untreated samples. In contrast, samples subjected to water adsorption, CEC, sedimentation volume, and methylene blue sorption did respond to the treatment.

The effects of steaming were generally influenced little if at all by the bentonite or clay type, whereas the interlayer cation of the smectite clearly had an influence in the case of hot water vapor. Moreover, a distinction between monovalent and divalent cations seems to be clearly visible in most of the tests.

As previously shown by Bish *et al.* (1997) and Madsen (1998), the XRD measurements revealed no differences between untreated and treated samples. The peak positions of different mineral phases remained unaffected by the steam treatment; minor changes in peak intensity can be explained easily by slight changes in particle orientation, packing density and instrumental conditions affecting absolute intensities. The mineralogical composition of samples (XRD) and the chemical environment of the species investigated (XPS) did not change due to the steam treatment.

Based on ^{27}Al NMR results, Bish *et al.* (1997) speculated about an attack on the octahedral sheet, resulting in a reduced proportion of octahedral Al after steam treatment. Regarding the disposition of octahedral Al, the authors assumed it to have relocated at the surface of the smectite particles. A relocation of the octahedral species seems unlikely in view of our XPS results. Such an attack-relocation mechanism would be detectable by XPS because the chemical environment of the element would change and so shift the band energies. The latter was not observed here. Note, however, that most of the peaks of the unprocessed sample show a smaller FWHM than peaks of the treated sample (Table 3). The FWHM values were interpreted in terms of crystallinity by Ebina *et al.* (1997) who reported decreasing FWHM with increasing crystallinity. A dependence of the FWHM of the O_{1s} and Al_{2p} peaks on the crystallinity of a given sample was also predicted by Mosser *et al.* (1992). Mapping these findings to the present situation implies that the treated samples are less crystalline than the untreated ones.

Based on the result that the chemistry and crystal structure of the samples were unchanged, only the surface characteristics of the particle could explain the differences observed. Phase transitions or structural transformations of the minerals present are unlikely, therefore.

The decreased sedimentation volume depended on temperature and, to a lesser extent, on moisture according to Oscarson and Dixon (1989) who related this effect to a decreased swelling capacity after steaming. The modification of SV and swelling capacity appeared at temperatures of 110ºC and increased with increasing temperature. The SV in the present study, however, was only measured after a 200ºC steam treatment but resulted in a decrease in SV also. As known, changes in SV are related to different electrokinetic charge properties at the particle surface, an aspect which will be discussed further in part II of this study.

In contrast to the findings of Oscarson and Dixon (1989) but in agreement with the results of Madsen (1998), the CEC values of K- and Na-smectites decreased by as much as 30% after the steam treatment, whereas the Mg- and Ca-smectites were identical, within a 10% error range (according to the findings of Dohrmann *et al.*, 2012). Theoretically, an isochemical growth of smectite particles should change the proportion of exchange sites stemming from the permanent layer charge relative to the variable charge sites on the *hk*0 faces. Hence, samples which show no particle growth should also show no changes in CEC. No systematic correlation was found between the change in CEC and the change in ESD. Neither does a direct comparison between ESD and CEC lead to a correlation.

The concentrations of the clay–water dispersion for the methylene blue (MB) spectra were identical for treated and untreated samples. Assuming that the density and diameter of the clay particles remained unchanged due to the treatment, the absolute clay surface available for methylene blue sorption is approximately equal for both treated and untreated samples. For this reason, the sorption kinetics of treated and untreated samples should be similar (Figure 7), which is true in terms of band positions but not in terms of absorption intensities. The kind of interlayer cation could be derived from the number of peaks and their positions and agreed with the results of Czímerová *et al.* (2004). The four band positions observed are related to the four different forms of MB in clay dispersion: larger or higher agglomerates: $(MB^+)_n$ – 577±4 nm, dimers: $(MB^+)_2$ – 614±9 nm, monomers: MB^+ – 675±6 nm, and the protonated form: MBH^{2+} or J-aggregates – 768±4 nm (Bujdák *et al.*, 2001). Changes in absorption intensity could probably be assigned to variations in layer charge for bands near 675±6 and 768±4 nm and charge density for the band near 577±4 nm (Bujdák *et al.*, 1998; Bujdák *et al.*, 2001). As previously indicated by CEC measurements and confirmed by MB spectra, the charge conditions of samples with a divalent interlayer cation remained unaffected, whereas samples with a monovalent cation showed a decrease in CEC and also a change in the MB spectra. These qualitative differences between mono- and divalent-loaded smectites are indicated by the results of time-dependent VIS spectra of methylene blue–clay interaction.

The ESD was expected to increase after the steam treatment. Dissolution and recrystallization processes in terms of Ostwald ripening (Eberl *et al.*, 1990) could occur due to enhanced temperature and pressure conditions in the autoclaves. The hydrothermal alteration of bentonite as a buffer material in nuclear-waste reposi-

https://doi.org/10.1346/CCMN.2014.0620303 Published online by Cambridge University Press

tories led to particle growth of clay particles (Pusch and Kasbohm, 2002). Another process that also leads to change in particle size is aggregation. Physical particle aggregation in partially saturated and heated clays might contribute to the decrease in swelling capacity (Oscarson and Dixon, 1989). In contrast to the findings of Pusch and Kasbohm (2002) and Oscarson and Dixon (1989), no systematic increase in the ESD upon hot-vapor treatment was found, possibly because the treatment times were insufficient or the temperatures not high enough. The effects of particle growth and particle aggregation could not be confirmed, therefore, under the experimental conditions in the present study.

From the water-adsorption measurements, two results are available: an absolute value after 24 h and rates for the water adsorption (Figure 4). To transfer the laboratory results into application in foundry technology and casting, only the rates of water adsorption are really important. Absolute values after 24 h are of little interest in terms of molding-sand preparation and regeneration because the time necessary for one casting cycle in serial production in a foundry is <<24 h (Grefhorst *et al.*, 2005). The absolute water adsorption or water-uptake capacity as well as the rate of water adsorption showed no clear difference between treated or untreated samples. The water-adsorption process depends on relative humidity, the interlayer cation, and on the amount of sample (Montes-H. and Geraud, 2004). Mechanical compaction of the sample plays a minor role and the drying temperature is irrelevant in terms of water adsorption. The relative humidity, amount of sample, drying temperature, and mechanical compaction were equal for both the untreated and treated samples. The influence of different interlayer cations on water adsorption was of great interest, however. As expected from Montes-H. *et al.* (2003), Montes-H. and Geraud (2004), and Kaufhold *et al.* (2010), the Na-loaded samples showed very high water-uptake capacities compared to those with a divalent interlayer cation. Samples saturated with Mg^{2+} and Ca^{2+} showed approximately equal amounts and rates, which agrees with the results of Montes-H. and Geraud (2004). As shown by Dontsova *et al.* (2004), the smaller and even more hydrated cations (Na^{+} and Mg^{2+}) lead to greater water sorption by the smectite than those with larger cations (K^{+} and Ca^{2+}). The amount of water adsorbed as well as the rates of adsorption were influenced by the interlayer cations in the order: $Na^{+} > K^{+} > Mg^{2+} > Ca^{2+}$ (Figure 4). The order of adsorption, depending on interlayer cation, varies from study to study (*i.e.* Montes-H. and Geraud, 2004; Dontsova *et al.*, 2004). A comparison of values from the present study with those of other studies is difficult, therefore. The correlation between CEC and water adsorption, as shown by Kaufhold *et al.* (2010), was not observed. After 30–60 min, however, the rates of water adsorption were equal and converged to zero (Figure 4) independent of sample, interlayer cation, and whether untreated/treated. Most of the water adsorbed had been taken up in the first minutes of the experiment, therefore, leading to the conclusion that the water adsorption has little or no influence on the molding-sand regeneration process or quality.

Unlike Al, increased Si concentrations in samples after the steam treatment were measured. Similar results, due to a hydrothermal treatment on MX-80 bentonite, were noted by Pusch (2000). During cooling of the samples after a hydrothermal treatment, silica from the surfaces of the clay particles was precipitated. This process caused superficial dissolution of smectite and accessory silicates and led to cementation and particle aggregation (Pusch, 2000) and might explain the increased Si concentrations.

In comparison to the Si concentrations measured in the blank experiments (1 g of sample immersed in 20 mL of water for 5 days), the concentrations of Si after steam treatment were rather low, however (see Table 2). This can be explained by noting that the transport of ionic species is more effective in a liquid medium than in a gaseous phase. In order to check if the measured Si concentrations in the blank experiments can be ascribed to the dissolution of smectite, the blank experiment of BeH Ca was modeled using *PhreeqC* (Parkhurst and Appelo, 1999) at pH 7. The calculated Si concentration is smaller than the measured concentration by a factor of six. Changing the pH to five does not affect this factor. These results suggest that the measured aqueous Si concentrations cannot be ascribed to the dissolution of smectite alone. Similar conclusions were reached by Baeyens and Bradbury (1997) who suggested that aqueous Si concentrations were controlled by the dissolution of quartz at circumneutral pH. Another potential source of Si is volcanic glasses altered during the alteration of the bentonites (Klinkenberg *et al.*, 2009). As volcanic glasses are amorphous, the recalculation of small amounts based on XRD analyses may not be possible. The suggestion that measured aqueous Si concentrations are not due to the dissolution of smectite is in accord with the observation that no structural changes took place due to the steam treatment.

Finally, changes in parameters (ESD, CEC, SV, and WA) showing differences between untreated and steam-treated samples is discussed. The parameters plotted show no correlation with each other and so no relation between them, measured or calculated, exists.

CONCLUSION AND FUTURE WORK

From the variety of comparative experiments performed, few revealed differences between untreated and steam-treated samples. On the basis of XRD and XPS results, steam treatment does not affect the internal structure of the minerals.

The reduced sedimentation volume observed for all samples after exposure to water vapor confirms success-

https://doi.org/10.1346/CCMN.2014.0620303 Published online by Cambridge University Press

ful steam treatment but did not allow us to identify the processes involved.

The measured changes in CEC are significant only in the case of monovalent interlayer cations, in contrast to the findings of Couture (1985) and Oscarson and Dixon (1989). The fact that CEC values of samples containing divalent interlayer cations do not change (within a 10% error margin) cannot be explained at present and requires further investigation. These differences between monovalent- and divalent-loaded smectites are also indicated by the results of time-dependent VIS spectra of methylene blue−clay interaction.

Realizing that sedimentation volume (see chapters 2 and 9 of Kruyt, 1952, for example) and CEC are influenced by the electrokinetic charge density and the surface-charge density, respectively, suggests that the differences observed in the present study are due to changes in the charge distribution at the surface of the minerals. This idea is in qualitative agreement with zeta potentials reported by Bish *et al.* (1997).

The likely negative influence of water vapor on the quality of the molding sand and on the sand-regeneration process could be due to the aforementioned results, but are not fully confirmed. Further experiments presented in part II of this study will include conductometric titrations as well as the determination of zeta potentials or electrophoretic mobilities as a function of pH. Furthermore, rheological measurements, which could be related directly to modifications in electrokinetic properties and changes in particle shape computed from conductometric titrations in particular (Dukhin and Derjaguin, 1974), will also be performed.

ACKNOWLEDGMENTS

The present research was funded within the special program ‘Geotechnologien’ (grant # 03G0707A) of the German Federal Ministry of Education and Research (BMBF). The authors thank S & B Industrial Minerals for supplying the bentonites and the Department of Engineering Geology and Hydrogeology RWTH for the opportunity to measure water adsorption. Finally, the authors thank the anonymous reviewers for their helpful comments and suggestions which improved the manuscript.

REFERENCES

Anthony, J.W., Bideaux, R.A., Bladh, K.W., and Nichols, M.C. (2013) *Handbook of Mineralogy*. Mineralogical Society of America, Chantilly, VA 20151-1110, USA. http://www.handbookofmineralogy.org/.

Ashmawy, A.K., El-Hajji, D., Sotelo, N., and Muhammad, N. (2002) Hydraulic performance of untreated and polymer-treated bentonite in inorganic landfill leachates. *Clays and Clay Minerals*, **50**, 546−552.

Baeyens, B. and Bradbury, M.H. (1997) A mechanistic description of Ni and Zn sorption on Na-montmorillonite. Part I: Titration and sorption measurements. *Journal of Contaminant Hydrology*, **27**, 199−222.

Baier, J. (1991) Griechischer Bentonit für Gießereien. *Giesserei*, **78**, 501−506.

Beeley, P. (2001) *Foundry Technology*. Butterworth-Heinemann, London, 719 pp.

Berghof (2012) Homepage of the Berghof company, http://www.berghof.com, visited on 15.01.2012.

Bergmann, J. and Kleeberg, R. (1998) Rietveld analysis of disordered layer silicates. *Materials Science Forum*, **278-2**, 300−305.

Bish, D.L., Wu, W., Carey, J.W., Costanzo, P., Giese, R.F., Earl, W., and Oss, C.J. (1997) Effects of steam on the surface properties of Na-smectite. *Proceedings of the 11th International Clay Conference: Clays for our Future*, Ottawa, pp. 569−575.

Bujdák, J., Janek, M., Madejová, J., and Komadel, P. (1998) Influence of the layer charge density of smectites on the interaction with methylene blue. *Journal of the Chemical Society, Faraday Transactions*, **94**, 3487−3492.

Bujdák, J., Janek, M., Madejová, J., and Komadel, P. (2001) Methylene blue interactions with reduced-charge smectites. *Clays and Clay Minerals*, **49**, 244−254.

Canesson, P. (1982) E.S.C.A. studies of clay minerals. Pp. 211−236 in: *Advanced Techniques for Clay Mineral Analysis* (J. Fripiat, editor). Developments in Sedimentology, **34**, Elsevier, Amsterdam.

Christidis, G.E. and Huff, W.D. (2009) Geological aspect and genesis of bentonites. *Elements*, **5**, 93−98.

Couture, R.A. (1985a) Steam rapidly reduces the swelling capacity of bentonite. *Nature*, **318**, 50−52.

Couture, R.A. (1985b) Rapid increases in permeability and porosity of bentonite-sand mixtures due to alteration by water vapor. *Materials Research Society Symposia Proceedings*, **44**, 515−522.

Czímerová, A., Jankovic, L., and Bujdák, J. (2004) Effect of exchangeable cations on the spectral properties of methylene blue in clay dispersions. *Journal of Colloid and Interface Science*, **274**, 126−132.

Dieng, M.A. (2005) Der Wasseraufnahmeversuch nach DIN 18132 in einem neu entwickelten Gerät. *Bautechnik*, **82**, 28−32.

DIN 6174 Farbmetrische Bestimmung von Farbmaβzahlen und Farbabständen im angenähert gleichförmigen CIELAB-Farbenraum. Ausgabe DIN 6174:2007-10.

Dohrmann, R., Genske, D., Karnland, O., Kaufhold, S., Kiviranta, L., Olsson, S., Plötze, M., Sandén, T., Sellin, P., Svensson, D., and Valter, M. (2012) Interlaboratory CEC and exchangeable cation study of bentonite buffer materials: I. Cu(II)-Triethylenentetramine method. C*lays and Clay Minerals*, **60**, 162−175.

Dontsova, K.M., Norton, D.L., Johnston, C.T., and Bigham, J.M. (2004) Influence of exchangeable cations on water adsorption by soil clays. *Soil Science Society of America Journal*, **68**, 1218−1227.

Dukhin, S.S. and Derjaguin, B.V. (1974) Equilibrium double layer and electrokinetic phenomena. Pp. 49−272 in: *Surface and Colloid Science* (E. Matijevic, editor). John Wiley & Sons, New York.

Eberl, D.D., Środoń, J., Kralik, M., Taylor, B.E., and Peterman, Z.E. (1990) Ostwald ripening of clays and metamorphic minerals. *Science*, **248**, 474−477.

Ebina, T., Iwasaki, T., Chatterjee, A., Katagiri, M., and Stucky, G.D. (1997) Comparative study of XPS and DFT with reference to the distributions of Al in tetrahedral and octahedral sheets of phyllosilicates. *Journal of Physical Chemistry B*, **101**, 1125−1129.

Erdoğan, B. and Demirci, Ş. (1996) Activation of some Turkish bentonites to improve their drilling fluid properties. *Applied Clay Science*, **10**, 401−410.

EUBA (European Bentonite Association) (2006) Position Paper, 10/2006, http://www.ima-europe.eu/sites/ima-europe.eu/files/publications/Bentonite_An-WEB-2011.pdf.

Fahrenholtz, W.G. (2008) Clays. Pp. 111–133 in: *Ceramic and Glass Materials: Structure, Properties and Processing* (J.F. Shackelford and R.H. Doremus, editors). Springer, Berlin.

Fairley, N. (2009) CasaXPS Manual – 2.3.15 Introduction to XPS and AES. Casa Software Ltd., 177p.

Gitipour, S., Bowers, M.T., and Bodocsi, A. (1997) The use of modified bentonite for removal of aromatic organics from contaminated soil. *Journal of Colloid and Interface Science*, **196**, 191–198.

Grefhorst, C. (2006) Prüfung von Bentoniten – Ausführliche Bewertung der Eigenschaften und ihr Wert für die Praxis. *Giesserei*, **93**, 26–31.

Grefhorst, C., Podobed, O., and Böhnke, S. (2005) Bentonitgebundene Formstoffe – Umlaufverhalten von Bentoniten unter besonderer Betrachtung des Kreislaufsystems und der Nasszugfestigkeit. *Giesserei*, **92**, 63–67.

Grim, R.G. and Güven, N. (1978) *Bentonites – Geology, Mineralogy, Properties and Uses*. Developments in Sedimentology **24**, Elsevier, Amsterdam.

Güven, N. (1990) Longevity of bentonite as buffer material in a nuclear-waste repository. *Engineering Geology*, **28**, 233–247.

Heuser, M., Andrieux, P., Petit, S., and Stanjek, H. (2013) Iron-bearing smectites: A revised relationship between structural Fe, *b* cell edge lengths and refractive indices. *Clay Minerals*, **48**, 97–103.

Jacobs, K.Y. and Schoonheydt, R.A. (2001) Time dependence of the spectra of methylene blue–clay mineral dispersions. *Langmuir*, **17**, 5150–5155.

Jordan, G., Eulenkamp, C., Calzada, E., Schillinger, B., Hoelzel, M., Gigler, A., Stanjek, H., and Schmahl, W.W. (2013) Quantitative in-situ study on the dehydration of bentonite bonded molding sands. *Clays and Clay Minerals*, **61**, 133–140.

Kahr, G. and Madsen, F.T. (1995) Determination of the cation exchange capacity and the surface area of bentonite, illite and kaolinite by methylene blue adsorption. *Applied Clay Science*, **9**, 327–336.

Kaufhold, S., Dohrmann, R., and Klinkenberg, M. (2010) Water-uptake capacity of bentonites. *Clays and Clay Minerals*, **58**, 37–43.

Klinkenberg, M., Rickertsen, N., Kaufhold, S., Dohrmann, R., and Siegesmund, S. (2009) Abrasivity by bentonite dispersions. *Applied Clay Science*, **46**, 37–42.

Köster, H.M. (1979) *Die chemische Silikatanalyse: Spektralphotometrische, komplexometrische und flammenspektrometrische Analysenmethoden.* Springer, Berlin, 212 pp.

Kruyt, H.R. (1952) *Colloid Science Volume 1 – Irreversible Systems*. Elsevier, Amsterdam.

Lagaly, G., Schulz, O., and Zimehl, R. (1997) *Dispersionen und Emulsionen. Einführung in die Kolloidik feinverteilter Stoffe einschließlich der Tonminerale*. 1st edition, Steinkopff-Verlag Darmstadt, Germany, pp. 285–289.

Lange, H. (1968) Bestimmung von Teilchengrößen aus Trübung und Brechungsinkrement. *Kolloid Zeitschrift und Zeitschrift für Polymere*, **223**, 24–30.

Lange, H. (1969) Bestimmung der Teilchengröße in ABS-Kunststoffen. *Kolloid Zeitschrift und Zeitschrift für Polymere*, **232**, 753–757.

Lange, H. (1995) Comparative test of methods to determine particle size and particle size distribution in the submicron range. *Particle and Particle Systems Characterization*, **12**, 148–157.

Luckham, P.F. and Rossi, S. (1999) The colloidal and rheological properties of bentonite dispersions. *Advances in Colloid and Interface Science*, **82**, 43–92.

Ma, Y.-L., Xu, Z.-R., Guo, T., and You, P. (2004) Adsorption of methylene blue on Cu(II)-exchanged montmorillonite. *Journal of Colloid and Interface Science*, **280**, 283–288.

Madsen, F.T. (1998) Clay mineralogical investigations related to nuclear waste disposal. *Clay Minerals*, **33**, 109–129.

Meier, L.P. and Kahr, G. (1999) Determination of the cation exchange capacity (CEC) of clay minerals using the complexes of copper (II) ion with triethylenetetramine and tetraethylenepentamine. *Clays and Clay Minerals*, **47**, 386–388.

Melik, D.H. and Fogler, H.S. (1983) Turbidimetric determination of particle size distributions of colloidal systems. *Journal of Colloid and Interface Science*, **92**, 161–180.

Mellah, A. and Chegrouche, S. (1997) The removal of zinc from aqueous solutions by natural bentonite. *Water Research*, **31**, 621–629.

Montes-H., G., and Geraud, Y. (2004) Sorption kinetics of water vapour of MX80 bentonite submitted to different physical–chemical and mechanical conditions. *Colloids and Surfaces A: Physicochemical and Engineering Aspects*, **235**, 17–23.

Montes-H., G., Duplay, J., Martinez, L., Geraud, Y., and Rousset-Tournier, B. (2003) Influence of interlayer cations on the water sorption and swelling-shrinkage of MX80 bentonite. *Applied Clay Science*, **23**, 309–321.

Mosser, C., Mosser, A., Romeo, M., Petit, S., and Decarreau, A. (1992) Natural and synthetic copper phyllosilicates studied by XPS. *Clays and Clay Minerals*, **40**, 1125–1129.

Murray, H.H. (2007) *Applied clay mineralogy – Occurrences, Processing and Application of Kaolins, Bentonites, Palygorskite-Sepiolite, and Common Clays*. Developments in Clay Science **2**, Elsevier, Amsterdam.

Neff, K.H. (1959) Über die Messung der Wasseraufnahme ungleichförmiger bindiger anorganischer Bodenarten in einer neuen Ausführung des Enslingerätes. *Die Bautechnik*, **39**, 415–421.

Oscarson, D.W. and Dixon, D.A. (1989) The effect of steam on montmorillonite. *Applied Clay Science*, **4**, 279–292.

Oscarson, D.W., Dixon, D.A., and Gray, M.N. (1990) Swelling capacity and permeability of an unprocessed and a processed bentonitic clay. *Engineering Geology*, **28**, 281–289.

Parkhurst, D.L. and Appelo, C.A.J. (1999) User′s Guide to PHREEQC (Version 2) A Computer Program for Speciation, Batch-Reaction, One-Dimensional Transport, and Inverse Geochemical Calculations. Water-Resources Investigations Report 99-4259, 312 pp. USGS Geological Survey, Denver, Colorado, USA.

Paterson, E. and Swaffield, R. (1994) X-ray photoelectron spectroscopy. Pp. 226–259 in: *Clay Mineralogy: Spectroscopic and Chemical Determinative Methods* (M.J. Wilson, editor). Chapman & Hall, London.

Pusch, R. (2000) On the effect of hot water vapor on MX-80 clay. Technical Report TR-00-16, SKB, 41 pp.

Pusch, R. and Kasbohm, J. (2002) Alteration of MX-80 by hydrothermal treatment under high salt content conditions. Technical Report TR-02-06, SKB, 39 pp.

Recknagel, U. and Dahlmann, M. (2008) Spezialsande-Formgrundstoffe für die moderne Kern- und Formherstellung. Hüttenes-Albertus, Düsseldorf, Germany.

Scalia, J. and Benson, C.H. (2011) Hydraulic conductivity of geosynthetic clay liners exhumed from landfill final covers with composite barriers. *Journal of Geotechnical and Geoenvironmental Engineering*, **137**, 1–13.

Träger, H. and Bührig-Polaczek, A. (2000) Foundry Technology. In: *Ullmann's Encyclopedia of Industrial Chemistry*. Wiley, New Jersey, USA.

Ufer, K., Stanjek, H., Roth, G., Dohrmann, R., Kleeberg, R., and Kaufhold, S. (2008) Quantitative phase analysis of bentonites by the Rietveld method. *Clays and Clay Minerals*, **56**, 272–282.

VDG P35 Prüfung von tongebundenen Formstoffen. Bestimmung des Anteils an bindefähigem Ton. 5 p., Okt. 1999.

Viraraghavan, T. and Alfaro, F. (1996) Adsorption of phenol from wastewater by peat, fly ash and bentonite. *Journal of Hazardous Materials*, **57**, 59–70.

Wojdyr, M. (2010) Fityk: a general-purpose peak fitting program. *Journal of Applied Crystallography*, **43**, 1126–1128.

Zhu, X., Jiang, D., and Tan, S. (2002) Preparation of silicon carbide reticulated porous ceramics. *Materials Science and Engineering A*, **323**, 232–238.

(*Received 9 April 2013; revised 25 July 2014; Ms. 757; AE: K. Emmerich*)